

# UC Irvine

## UC Irvine Previously Published Works

### Title

Summertime distribution of PAN and other reactive nitrogen species in the northern high-latitude atmosphere of eastern Canada

### Permalink

<https://escholarship.org/uc/item/13w3q4x8>

### Journal

Journal of Geophysical Research, 99(D1)

### ISSN

0148-0227

### Authors

Singh, HB  
Herlth, D  
O'Hara, D  
et al.

### Publication Date

1994-01-20

### DOI

10.1029/93jd00946

### Copyright Information

This work is made available under the terms of a Creative Commons Attribution License, available at <https://creativecommons.org/licenses/by/4.0/>

Peer reviewed

## Summertime distribution of PAN and other reactive nitrogen species in the northern high-latitude atmosphere of eastern Canada

H. B. Singh,<sup>1</sup> D. Herlth,<sup>1</sup> D. O'Hara,<sup>2</sup> K. Zahnle,<sup>1</sup> J. D. Bradshaw,<sup>3</sup>  
S. T. Sandholm,<sup>3</sup> R. Talbot,<sup>4</sup> G. L. Gregory,<sup>5</sup> G. W. Sachse,<sup>5</sup> D. R. Blake,<sup>6</sup>  
and S. C. Wofsy<sup>7</sup>

Aircraft measurements of key reactive nitrogen species (NO, NO<sub>2</sub>, HNO<sub>3</sub>, PAN, PPN, NO<sub>3</sub><sup>-</sup>, NO<sub>y</sub>), C<sub>1</sub> to C<sub>6</sub> hydrocarbons, acetone, O<sub>3</sub>, chemical tracers (C<sub>2</sub>Cl<sub>4</sub>, CO), and important meteorological parameters were performed over eastern Canada during July to August 1990 at altitudes between 0 and 6 km as part of an Arctic Boundary Layer Expedition (ABLE3B). In the free troposphere, PAN was found to be the single most abundant reactive nitrogen species constituting a major fraction of NO<sub>y</sub> and was significantly more abundant than NO<sub>x</sub> and HNO<sub>3</sub>. PAN and O<sub>3</sub> were well correlated both in their fine and gross structures. Compared to data previously collected in the Arctic/subarctic atmosphere over Alaska (ABLE3A), the lower troposphere (0-4 km) over eastern Canada was found to contain larger reactive nitrogen and anthropogenic tracer concentrations. At higher altitudes (4-6 km) the atmospheric composition was in many ways similar to what was seen over Alaska and supports the view that a large-scale reservoir of PAN (and NO<sub>y</sub>) is present in the upper troposphere over the entire Arctic/subarctic region. The reactive nitrogen budget based on missions conducted from the North Bay site (missions 2-10) showed a small shortfall, whereas the budget for data collected from the Goose Bay operation (missions 11-19) showed essential balance. It is calculated that 15-20 ppt of the observed NO<sub>x</sub> may find its source from the available PAN reservoir. Meteorological considerations as well as relationships between reactive nitrogen and tracer species suggest that the atmosphere over eastern Canada during summer is greatly influenced by forest fires and transported industrial pollution.

### INTRODUCTION

Northern high latitudes are of great interest to atmospheric scientists because of the high predicted sensitivity of this region to climatic change and the paucity of available data. Despite the remoteness of the Arctic/subarctic atmosphere, significant human influences are beginning to impact this region, especially in winter and early spring [Schnell, 1984; Rahn, 1985; Barrie, 1986; Jaffe *et al.*, 1991]. Only a few studies of the high-latitude environment have been conducted and these generally have focused on the winter/spring Arctic haze period. The NASA Global Tropospheric Experiment (GTE) seeks to understand the atmospheric chemistry associated with the earth's major ecosystems [McNeal *et al.*, 1983]. Recent GTE field measurements are now providing a large data base to investigate atmospheric photochemical and transport processes impacting the northern high latitudes. For example, aircraft flights during the Arctic Boundary Layer

Expedition3A (ABLE3A) provided measurements of a large number of reactive nitrogen species, ozone, hydrocarbons, anthropogenic tracers and important meteorological parameters over Alaska and Greenland during the summer (July to August) of 1988 [Harriss *et al.*, 1992]. Contrary to the commonly held view that the summer Arctic atmosphere is extremely clean [Barrie, 1986], this study showed that the Arctic/subarctic atmosphere was strongly affected by transported industrial pollution, high-latitude biomass burning, and incursions of stratospheric air [Sandholm *et al.*, 1992; Singh *et al.*, 1992a, b; Wofsy *et al.*, 1992a].

ABLE3B was a follow up field expedition to ABLE3A. While ABLE3A concentrated its efforts in Alaska to characterize the Arctic and North Pacific air masses prior to their transport across North America, the ABLE3B study moved to the midcontinent and eastern regions of Canada during the summer (July to August) of 1990. Details about the experimental plan and the general study objectives are presented in the overview paper by Harriss *et al.* [this issue]. Aircraft measurements of important reactive nitrogen species (NO, NO<sub>2</sub>, HNO<sub>3</sub>, PAN, PPN, NO<sub>3</sub><sup>-</sup>, NO<sub>y</sub>), O<sub>3</sub>, C<sub>1</sub> to C<sub>6</sub> hydrocarbons, acetone, aerosols, chemical tracers (C<sub>2</sub>Cl<sub>4</sub>, CO), and meteorological parameters were made. This paper and other complementary efforts [Sandholm *et al.*, this issue; Talbot *et al.*, this issue] describe various aspects of ABLE3B reactive nitrogen distributions and associated meteorology and compare these results with the previously published results from the Alaskan Arctic and subarctic atmosphere [Jacob *et al.*, 1992; Sandholm *et al.*, 1992; Singh *et al.*, 1992a, b].

<sup>1</sup>NASA Ames Research Center, Moffett Field, California.

<sup>2</sup>San Jose State University Foundation, Moffett Field, California

<sup>3</sup>Georgia Institute of Technology, Atlanta.

<sup>4</sup>University of New Hampshire, Durham.

<sup>5</sup>NASA Langley Research Center, Hampton, Virginia.

<sup>6</sup>University of California, Irvine.

<sup>7</sup>Harvard University, Cambridge, Massachusetts.

Copyright 1994 by the American Geophysical Union.

Paper number 93JD00946.  
0148-0227/94/93JD-00946\$05.00

## EXPERIMENTAL

ABLE3B utilized a Lockheed Electra for all airborne measurements. Instrument installation and flight tests were performed at Wallops Island, Virginia. Aircraft missions were conducted from July 5 to August 15, 1990, primarily from North Bay (46.3°N, 79.5°W) and Goose Bay (53.3°N, 60.4°W), Canada. Eight missions of approximately 5-hour duration were flown out of North Bay (NB) to the Hudson-James Bay lowlands (50°-60°N, 80°-95°W). In addition, 10 missions were conducted out of Goose Bay (GB) to the Schefferville (55°N, 67°W) area, including missions to and from Frobisher Bay on the southern tip of Baffin Island (63°N, 68°W). Field missions were divided into generic types that included boundary layer flux measurements, midtropospheric distributions, and vertical profiles to 6-km altitude. A latitude of 35°-65°N over 60°-95°W longitude was covered during this experiment. A map of the geographical extent covered during the ABLE3B missions and a summary table of individual flights are provided in the overview papers by *Harriss et al.* [this issue] and *Shipham et al.* [this issue].

An instrument named PANAK (PAN-aldehyde-ketone) was flown for the first time during the ABLE3B mission by investigators from the NASA Ames Research Center. The PANAK instrument was designed to measure PAN (also PPN and C<sub>2</sub>Cl<sub>4</sub>) and selected aldehydes and ketones using a pair of airborne gas chromatographs. Results based on the measurements of aldehydes and ketones are discussed in a companion paper [*Singh et al.*, this issue]. PAN was measured by electron-capture gas chromatography. With each PAN measurement it was also possible to simultaneously measure PPN and C<sub>2</sub>Cl<sub>4</sub>. Typically 150 ml of ambient air were collected through a window probe over a 90 s sampling period at a controlled -150°C temperature to obtain detection sensitivities of about 1 parts per trillion (ppt) for PAN, PPN, and C<sub>2</sub>Cl<sub>4</sub>. The experiment was substantially computer controlled and organic nitrogen analysis was performed every 6 min. PAN calibrations were performed by using a diffusion tube filled with liquid PAN in a *n*-tridecane matrix held at icewater temperature. Air was passed over the diffusion tube at a constant rate of flow to provide a calibration gas stream with PAN mixing ratios in the 10 to 20-ppb range. PAN in the exit stream was measured by using an NO<sub>y</sub> detector equipped with a molybdenum oxide converter held at 375°C. A nylon filter was inserted in line to remove any traces of nitric acid. Calibration of this chemiluminescence system was accomplished by using both NO<sub>2</sub> and NO standards that were intercompared with National Institute of Standards and Testing (NIST) primary standards. An on board dynamic dilution system was used to generate low parts per trillion mixing ratios of PAN. Instrument precision and accuracy are estimated to be ±10% and ±25%, respectively, at the 95% confidence level for PAN mixing ratios above 50 ppt. Details of this and similar techniques can be found elsewhere [*Singh and Salas*, 1983; *Joos et al.*, 1986; *Ridley et al.*, 1990; *Singh et al.*, 1990, 1992a].

NO, NO<sub>2</sub>, and NO<sub>y</sub> were measured by a laser-induced-fluorescence (LIF) instrument developed by *Sandholm et al.* [1990, 1992]. In this instrument the 226-nm and 1.1μm laser beams are colinearly combined and passed through three separate sample cells dedicated to ambient NO, NO<sub>2</sub>, and NO<sub>y</sub> detection. Measurement precision is estimated to be ±16% NO, ±20% NO<sub>2</sub>, and ±5% NO<sub>y</sub> for 3 min integration.

Absolute accuracy is estimated to be ±15% NO, ±18% NO<sub>2</sub>, and ±15% NO<sub>y</sub> (at the 95% confidence limit). Nitric acid (HNO<sub>3</sub>) was measured by the mist chamber technique described by *Talbot et al.* [1990]. A recent intercalibration of the mist chamber HNO<sub>3</sub> instrument with the National Oceanic and Atmospheric Administration (NOAA) nylon filter method and the National Center of Atmospheric Research (NCAR) Lind instrument showed agreement to within ±25% in the 100- to 1000-ppt range [*Atlas et al.*, 1992]. Sampling times varied from 3 to 45 min for HNO<sub>3</sub> with a limit of detection of 10 ppt. The overall uncertainty was estimated to be ±20% for concentrations ≥100 ppt increasing to ±30% for concentrations near the limit of detection (10 ppt). Instrumentation principles, sampling methods, sampling times, data precision and accuracy have been summarized in the overview paper by *Harris et al.* [this issue].

## RESULTS AND DISCUSSION

It is well known that nitrogen oxides play a central role in the chemistry of the atmosphere [*Levy*, 1971; *Crutzen*, 1979; *Logan et al.*, 1981]. Reactive nitrogen chemistry is complex and is strongly influenced by the presence of organic reservoir species [*Singh and Hanst*, 1981; *Calvert and Madronich*, 1987; *Singh*, 1987; *Kanakidou et al.*, 1991]. As stated earlier, a comprehensive set of reactive nitrogen measurements (NO, NO<sub>2</sub>, HNO<sub>3</sub>, PAN, PPN, NO<sub>3</sub><sup>-</sup> and NO<sub>y</sub>) were made during the ABLE3B deployment. Different sampling periods were employed in these measurements. Several merged files containing matching data averaged within the PAN, HNO<sub>3</sub>, and NO<sub>y</sub> sampling windows were created for the purposes of data analysis. Where fast response data were available (e.g., CO and O<sub>3</sub>) 1-min data averages were employed. For NO, NO<sub>2</sub>, and NO<sub>y</sub> both 1.5- and 3-min sampling sets were used. In the analysis and interpretation that follows, all of these data files were used as appropriate. Nitric acid sampling window was the longest and data merged to this window were used in all cases involving HNO<sub>3</sub>. Missions 2-10 are used to describe North Bay (NB) measurements, missions 11-19 are used to describe Goose Bay (GB) measurements, and missions 20-22 were transit flights terminating at Wallops Island, Virginia. Since both ABLE3A and ABLE3B sampled Arctic/subarctic air in summer, largely over Alaska and eastern Canada, comparisons are made to reveal important differences in the large-scale atmospheric chemical structures.

The atmospheric composition of air over central/eastern Canada during ABLE3B was impacted by a variety of air masses containing forest fire smoke, industrial pollution, and stratospheric air. According to the meteorological classification for the first 18 ABLE3B missions, provided by *Shipham et al.* [this issue], forest fires impacted missions 4-9, 11-13, and 15-18, pollution possibly affected missions 4, 5, 10, 13, 16 and 17, and stratospheric influences could be seen in upper layers during missions 1-3, 5, 7-9, 12, 14, 16-18. Forest fires were both local (missions 7-9, 11) as well as remote (missions 4-7, 11-13, 15-17). Mission 6 provided a dramatic example of the influence of haze and smoke plumes transported over long distances and has been discussed in some detail by *Shipham et al.* [this issue]. High C<sub>2</sub>Cl<sub>4</sub> mixing ratios further indicated that mission 11 was impacted by pollution as well but the flow of air was from the Northwest Atlantic. It is worth pointing out that C<sub>2</sub>Cl<sub>4</sub> and CCl<sub>3</sub>F (CFC

11), conventional tracers of urban pollution, were often inconclusive indicators although some enhancement in  $C_2Cl_4$  could be seen in missions 10, 11, 13, 16, and 20-22. The reason for this was that small source signatures superimposed on a large background could not be easily separated. In rare instances (upper levels in missions 14, 15, 17), Pacific air of mixed tropical/mid-latitude origin was also sampled. In short the atmosphere over central/eastern Canada was strongly influenced by a variety of complex sources. A further discussion of selected events has been provided by *Browell et al.* [this issue], *Shipham et al.* [this issue], *Singh et al.* [this issue], and *Wofsy et al.* [this issue].

#### Atmospheric Distributions: Mixing Ratios, Variabilities and Vertical Structures

Figure 1a shows the mean, minimum, and maximum mixing ratios of PAN measured during each of the ABLE3B missions. Mixing ratios for missions 2-10 (NB) and 11-19 (GB) are mostly in the range of 100-300 ppt with one mission in the NB series (mission 6) showing a mean PAN concentration of about 400 ppt. This value involved measurements in elevated haze and smoke plumes presumed to originate from biomass

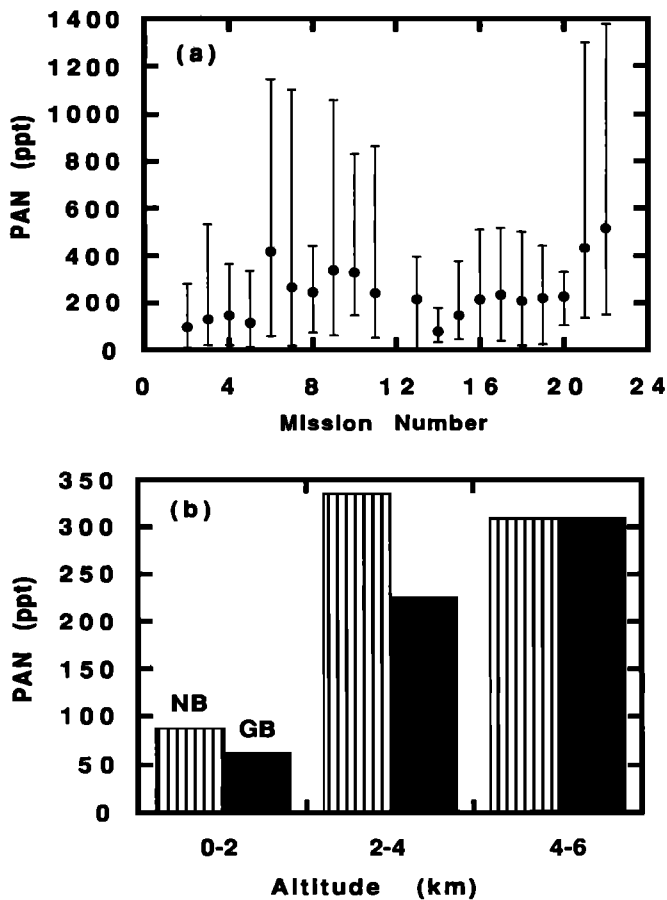


Fig. 1. PAN mixing ratios during ABLE3B. (a) Circles show mean PAN mixing ratios ( $\text{ppt}=10^{-12}$  v/v) for each mission; vertical lines indicate maximum and minimum measured values. (b) Mean PAN mixing ratios in the mean spell out (PBL) (0-2 km), transition layer (2-4 km), and free tropospheric layer (4-6 km) for North Bay (missions 2-10) and Goose Bay (missions 11-19) flights. In all subsequent figures, North Bay (NB, 46°N) and Goose Bay (GB, 53°N) represent data from these identified missions.

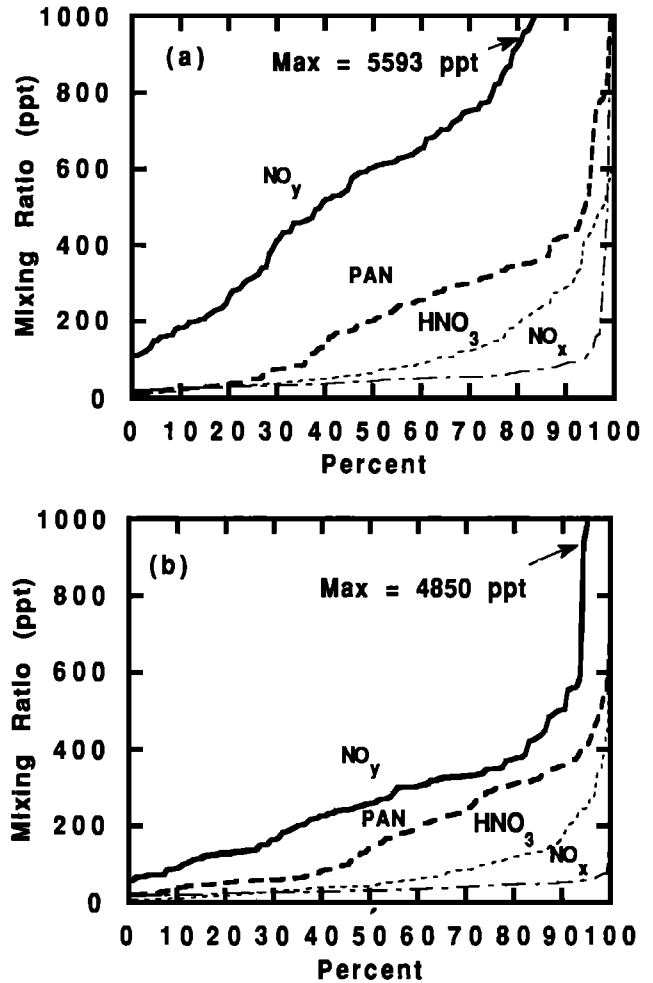


Fig. 2. Cumulative frequency distribution of mixing ratio for  $NO_y$ , PAN,  $HNO_3$ , and  $NO_x$  measured during (a) NB and (b) GB flights.

burning and distant Alaska fires [*Shipham et al.*, this issue]. The two transit flights back to the United States (missions 21 and 22) also show a mean PAN concentration exceeding 400 ppt and maximum values exceeding 1200 ppt because of their proximity to anthropogenic sources.

The aircraft vertical profiles for the NB and GB missions were examined to determine the height of the planetary boundary layer (PBL). Using the measurements of air temperature, dew point, and potential temperature, the PBL varied from 1500 to 3000 m with a mean height and standard deviation of  $2137 \pm 651$  m for NB and  $2193 \pm 361$  m for GB. On the basis of this analysis, Figure 1b shows mean PAN mixing ratios for the 0-to 2-km mean PBL, the 2-to 4-km transition layer, and the 4-to 6-km free tropospheric layer. Mean mixing ratios in the PBL and transition layers are larger for the NB missions toward James Bay than for the Labrador missions to Schefferville and toward Frobisher Bay (GB). Free tropospheric values (4-6 km), however, are comparable. This supports the contention that the northern high-latitude upper troposphere is a relatively uniform, large-scale PAN reservoir [*Singh et al.*, 1992a].

Figure 2 shows cumulative frequency distributions of mixing ratios for  $NO_y$ , PAN,  $HNO_3$ , and  $NO_x$  measured during NB and GB flights. Nearly 80% of the measurements for the NB missions fell in the range of 20-350 ppt for PAN, 100-

TABLE 1. Characteristic Weather Patterns Over Eastern Canada During the Arctic Boundary Layer Expedition (ABLE3B)

Mission	Position of 700 mbar Polar Vortex	Direction of Synoptic flow	Air Mass Character	Air Mass Origin
2, 3 (NB)	over or east of Hudson Bay	northerly	Arctic	Arctic islands
5, 6, 7 (NB)	north/NW of Hudson Bay	northwesterly	continental polar	western Canada/Alaska
4, 8, 9, 10 (NB)	far north of Hudson Bay	southwesterly to southerly	maritime polar/maritime subtropical	central/western United States
11, 14, 18, 19 (GB)	north of Hudson Bay	northwesterly to westerly	continental polar	northern Canada
13, 15, 16, 17 (GB)	north of Arctic circle	southwesterly to southerly	maritime polar	central/eastern United States

\* NB, North Bay; GB, Goose Bay.

900 ppt for  $\text{NO}_y$ , 20-60 ppt for  $\text{NO}_x$ , and 10-200 ppt for  $\text{HNO}_3$ . These numbers are smaller for the GB missions, especially for  $\text{NO}_y$  (60-400 ppt) and  $\text{HNO}_3$  (10-125 ppt). Also, 17% of the  $\text{NO}_y$  data for the NB missions exceeded 1000 ppt, whereas only 5% of the GB series exceeded this value. Figures 1 and 2 show that mixing ratios sampled in the Hudson Bay lowlands during the NB missions were generally higher than those obtained in the Labrador area during the GB missions.

The meteorological conditions that prevailed during ABLE3B were examined to assess their impact on measurements from different air masses and wind (air trajectory) patterns [Shipham *et al.*, this issue]. Using height contour analyses of the lower troposphere 700 mbar (3 km msl) constant pressure surface, several characteristic weather patterns were recognized. Table 1 lists the principal features of these patterns and the mission numbers to which they apply. Typically, the prevailing synoptic patterns pointed to the flow of Arctic/subarctic air from north to northwest and the flow of potentially anthropogenically perturbed air from the south to southwest. Generally, clean conditions were encountered during northerly flow of Arctic air and NW flow of polar air except for intermittent low-level smoke and haze layers (e.g., mission 6). Figure 3 shows the vertical distribution of PAN,  $\text{HNO}_3$ , and  $\text{O}_3$  for NB missions 5 and 9. The vertical profiles are obtained by using the available measurements of PAN,  $\text{HNO}_3$  (15-min sampling time), and  $\text{O}_3$  (3-min sampling time) for one ascent and one descent made during mission 5 and for two ascents and two descents made during mission 9. The profile data were obtained between Moosonee and Churchill for mission 5 and between North Bay and Moosonee for mission 9. Lines connecting the PAN and  $\text{HNO}_3$  data points are drawn for visual aid. Mission 5 is characteristic of clean NW flow, whereas mission 9 represents S-SW flow. Mission 5 was downwind of distant fires in Alaska and may have been minimally impacted. However, local fires did influence mission 9 at low altitudes and biomass burning was visible during the mission. Tropospheric (2-6 km)  $\text{C}_2\text{Cl}_4$  mixing ratios (not shown) were also slightly larger during mission 9 ( $11 \pm 3$  ppt) compared to mission 5 ( $9 \pm 1$  ppt). (If the data are assumed to have a normal Gaussian distribution, the probability of finding  $\text{C}_2\text{Cl}_4$  mixing ratios of  $\geq 11$  ppt would be 50% in the case of mission 9 but only 2% in the case of mission 5.) In Figure 3b and 3c the combined affect of forest fires and pollution is seen in the enhanced mixing ratios of  $\text{HNO}_3$  and  $\text{O}_3$  below 1-km altitude observed during mission 9. Figure 4 shows

similar behavior for selected GB missions (missions 14 and 17), that included several ascents and descents in the same geographical area of Schefferville, illustrating the impact of southerly flow on PAN and  $\text{O}_3$ . During mission 14, air trajectories in the midtroposphere came from the west-northwest across the Hudson Bay and may have been over the Pacific 10-15 days prior, while during mission 17 they came from a southwesterly direction across the North Bay area. Once again, whereas mission 14 was free of forest fires, mission 17 was impacted by both pollution and upwind fires from Alaska. Upper level (4-6 km)  $\text{C}_2\text{Cl}_4$  concentrations were significantly larger during mission 17 ( $16 \pm 3$  ppt) compared to mission 14 ( $12 \pm 2$  ppt) (also see Singh *et al.*, [this issue]). In both study areas during ABLE3B pollution episodes were often superimposed on forest fires. No data on any unique tracers of forest fire plumes (e.g.,  $\text{CH}_3\text{Cl}$ ) were available.

Figure 5 shows all NB and GB measurements of PAN,  $\text{NO}_y$ , and  $\text{O}_3$  plotted as a function of altitude. The high data points at 3 km-altitude and above are associated with the presence of haze and smoke layers, pollution episodes, and in some cases, stratospheric intrusions. For example, in Figure 5b the PAN measurements above 600 ppt were all encountered during mission 11 when air impacted with smoke was sampled. Similarly, noted outliers in Figure 5a are all from missions 6 and 9 sampling air masses mixed with smoke plumes, and mission 10 sampling polluted air in turbulent cloudy weather. The situation with  $\text{NO}_y$  outliers is virtually identical. Figure 6 shows the vertical distribution of PAN,  $\text{NO}_x$ , and  $\text{NO}_y$  for the GB missions which have been filtered to exclude some obvious cases of pollution episodes ( $\text{CO} < 105$  parts per billion (ppb)). Neglecting the outliers, the odd nitrogen species and  $\text{O}_3$  show an increase with height similar to that observed over the Arctic/subarctic region sampled over Alaska [Singh *et al.*, 1992a, b]. Details of the  $\text{O}_3$  distribution over eastern Canada have been provided by Anderson *et al.* [this issue]. Table 2 lists mean mixing ratios ( $\pm 1\sigma$ ) of species measured during ABLE3A and ABLE3B for the mean boundary layer (0-2 km), the transition layer (2-4 km), and the free tropospheric layer (4-6 km). Median mixing ratios are shown in Figure 7 for easy comparison. The measurements represent those made at the primary sites of Barrow and Bethel, Alaska, and North Bay and Goose Bay, Canada. Some of the salient differences are noted as follows:

1. In the boundary layer, mean (or median) mixing ratios of PAN for the NB and GB missions were larger than those for the Alaska missions. At the free tropospheric altitudes of 4-6 km, PAN mixing ratios were comparable at all sites and

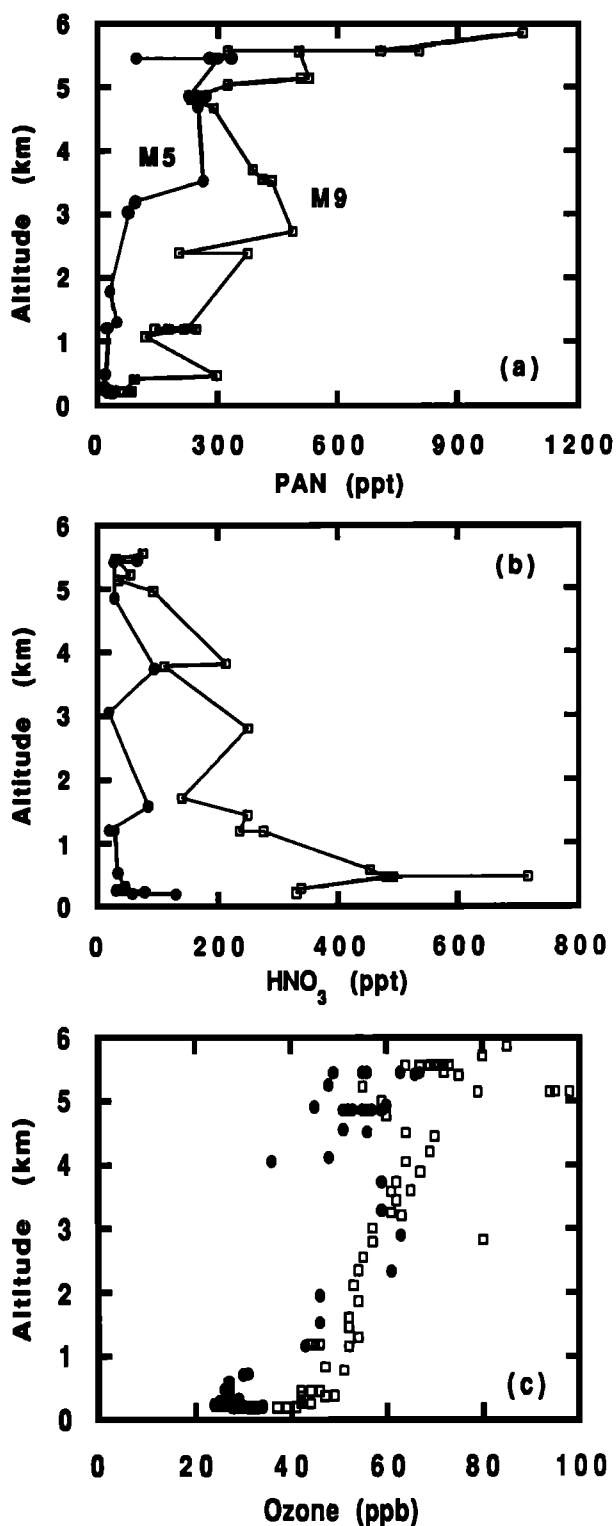


Fig. 3. Vertical profiles of ambient air mixing ratios of PAN, HNO<sub>3</sub>, and O<sub>3</sub> as measured during NB missions 5 (circles) and 9 (squares). The profiles correspond to conditions of clean NW (mission 5) and polluted S-SW (mission 9) flow.

were always significantly larger than the surface values. Large variability was observed in the transition layer (2-4 km) especially for NB and GB. The largest variations occurred during missions that were impacted by haze, forest fire, and pollution plumes.

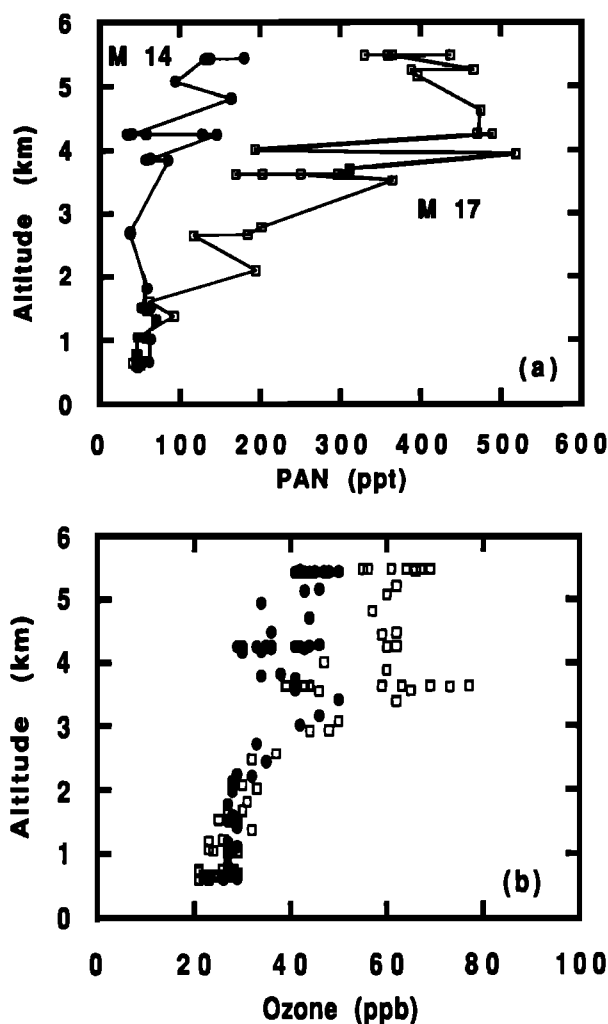


Fig. 4. Vertical profiles of ambient air mixing ratios of PAN and O<sub>3</sub> as measured during GB missions 14 (circles) and 17 (squares). The profiles correspond to conditions of clean W-NW (mission 14) and polluted S-SW (mission 17) flow.

2. Mean (or median) NO<sub>y</sub> mixing ratios were highest at NB and lowest at GB. This behavior was also reflected in the O<sub>3</sub>/NO<sub>y</sub> ratios (Table 3). Standard deviations in the 2- to 4-km and 4- to 6-km layers were very large during the GB missions.

3. NO<sub>x</sub> values in the various tropospheric layers are comparable, except for the NB missions when mixing ratios were relatively large in the lower troposphere (0-4 km) with considerable variability. Unlike NO<sub>y</sub> however, NO<sub>x</sub> mixing ratios at GB were not the lowest, and at high altitudes (4-6 km) were comparable to those at NB. In this respect NO<sub>x</sub> behavior was similar to that of PAN, CO and C<sub>2</sub>H<sub>2</sub>.

4. Despite substantial variabilities, HNO<sub>3</sub>, CO, and C<sub>2</sub>H<sub>2</sub> show significantly higher mixing ratios in the boundary and transition layers for the NB missions compared to other sites. Ozone values, on the other hand, are quite comparable for all altitude layers at all sites.

Overall, the atmosphere over eastern Canada during ABLE3B was perturbed by forest fires and surface pollution plumes significantly more than over Alaska (ABLE3A). These measurements did, however, confirm the existence of the large-scale upper tropospheric PAN (and NO<sub>y</sub>) reservoir in the

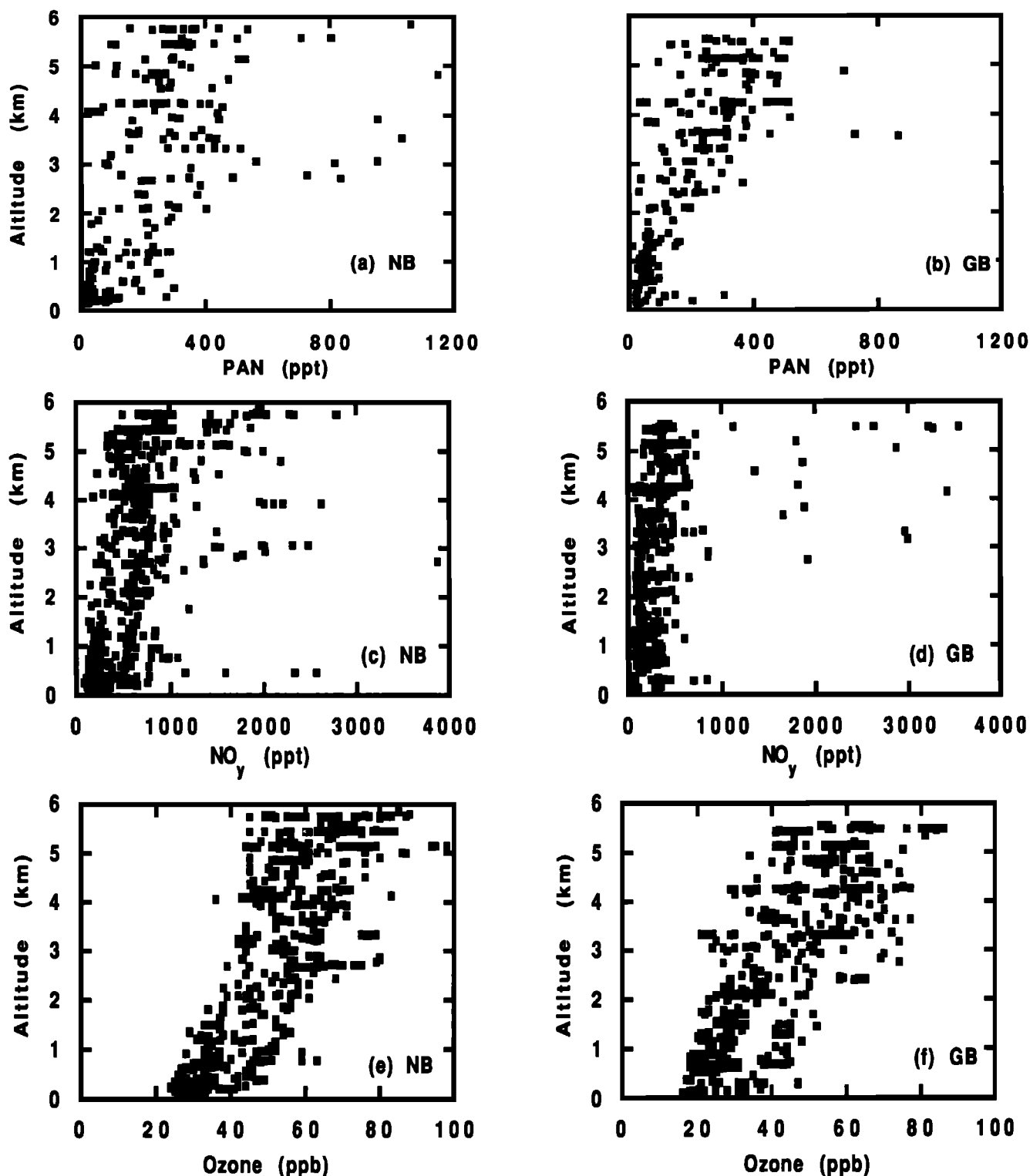


Fig. 5. (a, c, e) Vertical distribution of PAN,  $\text{NO}_y$ , and  $\text{O}_3$  in the troposphere of eastern Canada for all NB and (b, d, f) GB ABLE3B missions.  $\text{NO}_y$  and  $\text{O}_3$  data are 3-min averages. High data points at 3 km and above indicate measurements influenced by haze, pollution, and fire plumes.

Arctic/subarctic atmosphere as postulated from the Alaskan measurements [Sandholm *et al.*, 1992; Singh *et al.*, 1992a, b].

#### $\text{PAN}/\text{NO}_x$ , $\text{PAN}/\text{NO}_y$ , and $\text{PAN}/\text{HNO}_3$ Ratios

Figure 8 shows vertical distributions of  $\text{PAN}/\text{NO}_x$ ,  $\text{PAN}/\text{NO}_y$ , and  $\text{PAN}/\text{HNO}_3$  ratios for NB and GB data sets. In

all cases, larger ratios occurred at the higher altitudes in large part due to the rapidly increasing PAN mixing ratios.  $\text{PAN}/\text{NO}_x$  ratios increased to a nominal value of about 10 between 4 and 6 km although isolated values of 20–30 were also present in the NB data. In general, these ratios were smaller during ABLE3B than those seen in ABLE3A in part because of higher  $\text{NO}_x$  values encountered during ABLE3B.

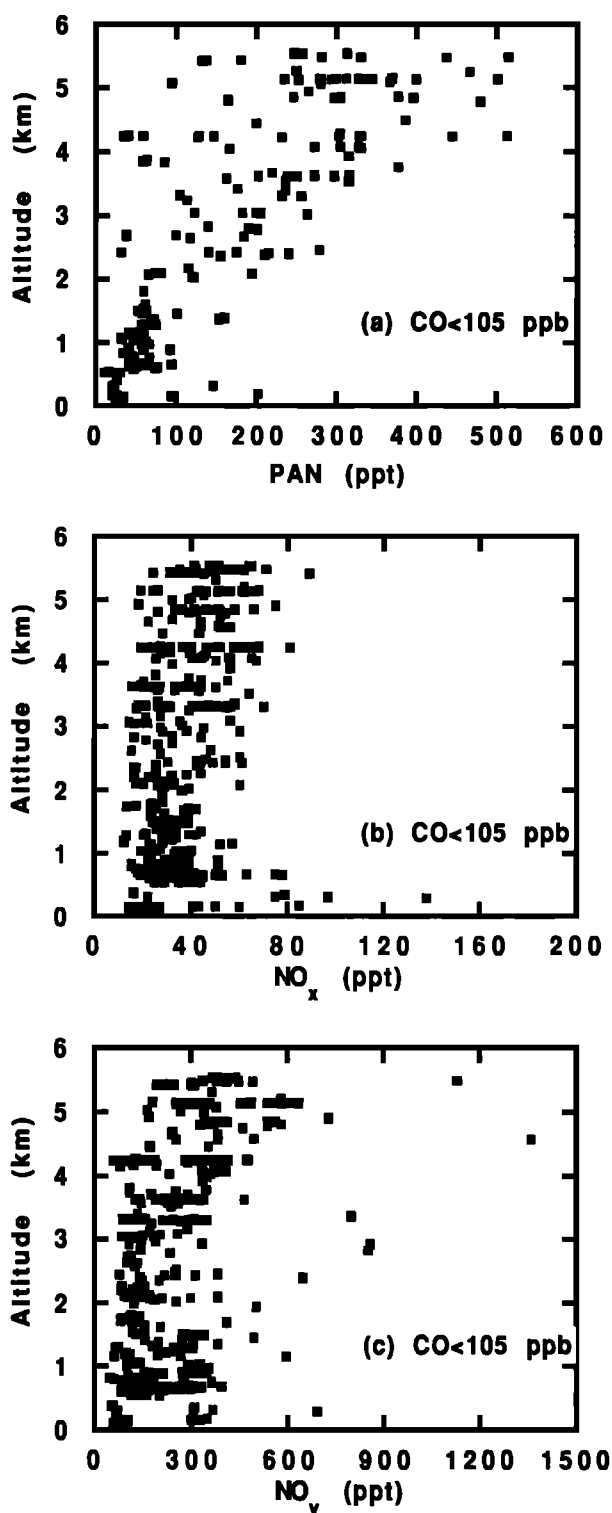


Fig. 6. Vertical distribution of PAN,  $\text{NO}_x$ , and  $\text{NO}_y$  for GB missions under clean conditions. Clean air is defined with a CO filter of <105 parts per billion (ppb).

Based on the best analysis of the data, it can be stated that the PAN/ $\text{NO}_y$  ratios at NB were typical of what was seen in Alaska, but the corresponding GB ratios are significantly larger. Sporadic cases where PAN/ $\text{NO}_y$  ratio exceeded 1 were first encountered during mission 16 and persisted through mission 23. Sandholm *et al.* [this issue] note that the  $\text{NO}_y$  converter lost its efficiency sometime during mission 21 but

operated normally prior to that. There were instances (e.g., mission 16) where both PAN and  $\text{HNO}_3$  independently exceeded measured  $\text{NO}_y$ . In general, these exceedances were within the uncertainties of the individual measurements. No such cases were encountered either at NB or at experiments performed in Alaska [Sandholm *et al.*, 1992; Singh *et al.*, 1992b]. It is also evident from Figure 8 that PAN mixing ratios significantly greater than  $\text{HNO}_3$  were frequently encountered over eastern Canada.

#### Relationships Between Reactive Nitrogen and Tracer Species

The relationships between PAN,  $\text{NO}_y$ , CO,  $\text{O}_3$ , select hydrocarbons, and  $\text{C}_2\text{Cl}_4$  were explored to see if these can shed any light on the nature of reactive nitrogen sources. Figure 9 shows that, in general, high PAN values, both in the boundary layer and aloft, are associated with correspondingly high values of CO,  $\text{C}_2\text{H}_2$  and  $\text{NO}_y$ . Linear correlation coefficients ( $R$ ) in the vicinity of 0.7 are calculated. Several of the high correlations such as those in Figures 9b, 9c, and 9d are the result of high concentration values measured above 2 km in polluted air. For example, the three data points (PAN > 600 ppt) in Figure 9b and the two data points (PAN > 600 ppt) in Figure 9d were measured during GB mission 11 when polluted air was sampled in turbulent cloudy weather (see also Figure 5). Similarly, the high concentration data points in Figure 9c were associated with missions affected by smoke and haze layers (e.g., NB mission 6). Although  $\text{C}_2\text{Cl}_4$  data showed the existence of sporadic pollution, it was not possible to find distinct correlations among PAN,  $\text{NO}_y$ , and  $\text{C}_2\text{Cl}_4$  largely because of the extremely small variability in  $\text{C}_2\text{Cl}_4$  mixing ratios. Both CO and  $\text{C}_2\text{H}_2$  are tracers of biomass burning and urban air pollution. As stated earlier, no unique tracers of biomass burning (possibly  $\text{CH}_3\text{Cl}$ ) were measured. Figure 9 is largely consistent with the view, also supported by meteorological analysis, that both forest fires and pollution impacted this region.

PAN was also correlated with  $\text{O}_3$  both in the boundary layer and aloft (Figure 10) in a manner similar to that observed over Alaska [Singh *et al.*, 1992a]. The correlation at GB was somewhat stronger than that at NB. In NB, because of the influence of smoke plumes, a greater scatter in the data is seen. However, when such cases are excluded the PAN- $\text{O}_3$  correlation at NB is comparable to that at GB. These PAN- $\text{O}_3$  relationships are indicative of the influences of continental precursors [Singh *et al.*, 1990, 1992a]. The  $\text{NO}_y$ - $\text{O}_3$  correlations are also shown. It is noteworthy that the mean  $\text{NO}_y$  mixing ratios at GB are much smaller than those at NB for a comparable amount of  $\text{O}_3$ . Mean  $\text{O}_3/\text{NO}_y$  ratios at NB ( $107 \pm 54$ ) were about 40% smaller than at GB ( $179 \pm 86$ ). This behavior was observed at all altitudes but was more significant in the free troposphere (Table 3). It is noted that  $\text{O}_3/\text{NO}_y$  ratios observed here and over Alaska [Singh *et al.*, 1992b] are significantly smaller than those observed in the lower stratosphere [Murphy *et al.*, 1993]. This provides little support for the suggestion made by Jacob *et al.* [1992] that stratospheric transport may provide a large source of Arctic/subarctic reactive nitrogen.

#### Budget of Reactive Nitrogen Species

Issues relating to reactive nitrogen budget, shortfall and the associated variability have been studied in detail by Sandholm



TABLE 2. Mean Mixing Ratios and Standard Deviations of Trace Species Measured Over Eastern Canada and Alaska

Location	Altitude Range, km	NO <sub>y</sub> ,* ppt	PAN, ppt	HNO <sub>3</sub> , ppt	NO <sub>x</sub> , ppt	O <sub>3</sub> , ppb	CO, ppb	C <sub>2</sub> H <sub>2</sub> , ppt	C <sub>2</sub> Cl <sub>4</sub> , ppt
North Bay (missions 2 - 10)	0 - 2	363 ±304†	88 ±83	140 ±147	63 ±107	36 ±8	125 ±27	142 ±107	11 ±2
	2 - 4	825 ±624	336 ±217	171 ±148	79 ±219	57 ±10	149 ±65	235 ±198	12 ±3
	4 - 6	860 ±468	310 ±193	72 ±90	42 ±17	62 ±12	110 ±25	118 ±75	12 ±4
Goose Bay (Missions 11 - 19)	0 - 2	204 ±118	63 ±45	112 ±140	36 ±19	29 ±9	103 ±23	88 ±51	13 ±2
	2 - 4	330 ±402	226 ±137	72 ±57	36 ±13	46 ±13	107 ±23	99 ±55	12 ±2
	4 - 6	525 ±684	310 ±123	45 ±31	44 ±14	57 ±12	105 ±41	118 ±115	13 ±2
Barrow, Alaska (Missions 6-13)	0 - 2	366 ±244	25 ±29	64 ±53	31 ±43	36 ±10	70 ±5	47 ±13	12 ±1
	2 - 4	501 ±211	141 ±71	37 ±30	24 ±10	63 ±13	73 ±4	59 ±13	13 ±2
	4 - 6	775 ±364	274 ±94	26 ±6	32 ±14	79 ±28	75 ±4	83 ±30	14 ±2
Bethel, Alaska (Missions 14-26)	0 - 2	325 ±210	31 ±19	65 ±42	31 ±24	35 ±8	80 ±12	62 ±22	10 ±2
	2 - 4	636 ±319	141 ±90	76 ±70	24 ±13	61 ±10	86 ±18	81 ±47	11 ±1
	4 - 6	732 ±287	304 ±117	129 ±114	32 ±12	76 ±10	90 ±17	99 ±50	12 ±2

\*For North Bay and Goose Bay, NO<sub>y</sub>, NO<sub>x</sub> and O<sub>3</sub> mean concentrations are calculated from the NO<sub>y</sub> file containing 3-min data. PAN data are based on direct measurements (PAN file). All other data are computed from the merged HNO<sub>3</sub> data file.

†Mean ± one standard deviation

*et al.* [this issue]. The data used in this section is exclusively merged to the HNO<sub>3</sub> sampling window. Table 3 summarizes the partitioning of odd nitrogen species and ozone relative to measured NO<sub>y</sub> in 2-km altitude bands. The quantity NO<sub>yi</sub> is defined as the sum of the observed gaseous odd nitrogen species (NO<sub>yi</sub>=NO+NO<sub>2</sub>+PAN+PPN+HNO<sub>3</sub>). PPN was present in extremely small and often undetectable concentrations. Although small amounts of aerosol nitrate were present (about 5% of NO<sub>y</sub>), only the fine aerosol fraction was probably sampled by the aircraft NO<sub>y</sub> instrument. No size fractionated aerosol measurements were done. Previous studies from remote clean air have shown that a substantial fraction of nitrate aerosols are generally found in the coarse fraction (e.g., crustal materials). Hence, aerosol NO<sub>3</sub><sup>-</sup> is not included in the definition of NO<sub>yi</sub>. To the extent that some aerosol nitrate

may be sampled as NO<sub>y</sub>, a small error is possible. As expected, PAN is the dominant NO<sub>y</sub> species in the upper troposphere (4-6 km), whereas HNO<sub>3</sub> dominates in the boundary layer for both NB and GB measurements. On average (Table 3), NO<sub>yi</sub> is nearly always less than NO<sub>y</sub> in NB and accounts for 55 to 77% of measured NO<sub>y</sub>. Some 100-400 ppt of reactive nitrogen is unaccounted for.

In GB the picture is quite different and NO<sub>yi</sub> accounts for nearly all of NO<sub>y</sub> and actually exceeds it by a small amount in some instances (Table 3). Given the error bars in individual measurements and the inexact overlapping of sampling windows, it is not surprising for NO<sub>yi</sub> to exceed NO<sub>y</sub> some of the time. What is surprising is that this result (NO<sub>yi</sub> = NO<sub>y</sub>) is contrary to what was seen at NB where similar air masses were sampled, and in Alaska. Indeed, reactive nitrogen

TABLE 3. Odd Nitrogen Partitioning Over Eastern Canada During ABLE3B

Location	Altitude Range, km	O <sub>3</sub> /NO <sub>y</sub>	NO <sub>x</sub> /NO <sub>y</sub>	HNO <sub>3</sub> /NO <sub>y</sub>	NO <sub>3</sub> <sup>-</sup> /NO <sub>y</sub>	PAN/NO <sub>y</sub>	NO <sub>yi</sub> <sup>+</sup> /NO <sub>y</sub>	NO <sub>y</sub> -NO <sub>yi</sub> , ppt
North Bay (missions 2 - 10)	0 - 2	138±64 (232)†	0.17±0.06 (58)	0.33±0.20 (58)	0.05±0.03 (16)	0.22±0.11 (52)	0.70±0.23 (52)	94±77 (52)
	2 - 4	91±39 (143)	0.09±0.09 (26)	0.22±0.12 (28)	0.05±0.05 (7)	0.43±0.13 (26)	0.77±0.18 (24)	235±317 (24)
	4 - 6	85±30 (222)	0.06±0.02 (35)	0.09±0.09 (37)	0.04±0.08 (6)	0.38±0.18 (36)	0.54±0.21 (34)	427±370 (34)
Goose Bay (missions 11 - 19)	0 - 2	175±85 (187)	0.21±0.09 (55)	0.52±0.44 (55)	0.06±0.04 (13)	0.39±0.24 (51)	1.13±0.50 (51)	-10±105 (51)
	2 - 4	201±98 (155)	0.15±0.07 (32)	0.29±0.26 (33)	0.04±0.02 (5)	0.77±0.31 (27)	1.19±0.44 (26)	-14±155 (26)
	4 - 6	163±70 (175)	0.11±0.06 (35)	0.11±0.09 (35)	0.02±0.01 (8)	0.76±0.27 (33)	1.00±0.32 (33)	184±777 (33)

\* Aerosol nitrate is expected to be largely present in the coarse fraction which is probably not sampled by the NO<sub>y</sub> instrument.

<sup>+</sup>NO<sub>yi</sub> = NO + NO<sub>2</sub> + PAN + PPN + HNO<sub>3</sub>

†Mean ± one standard deviation (number of data points).

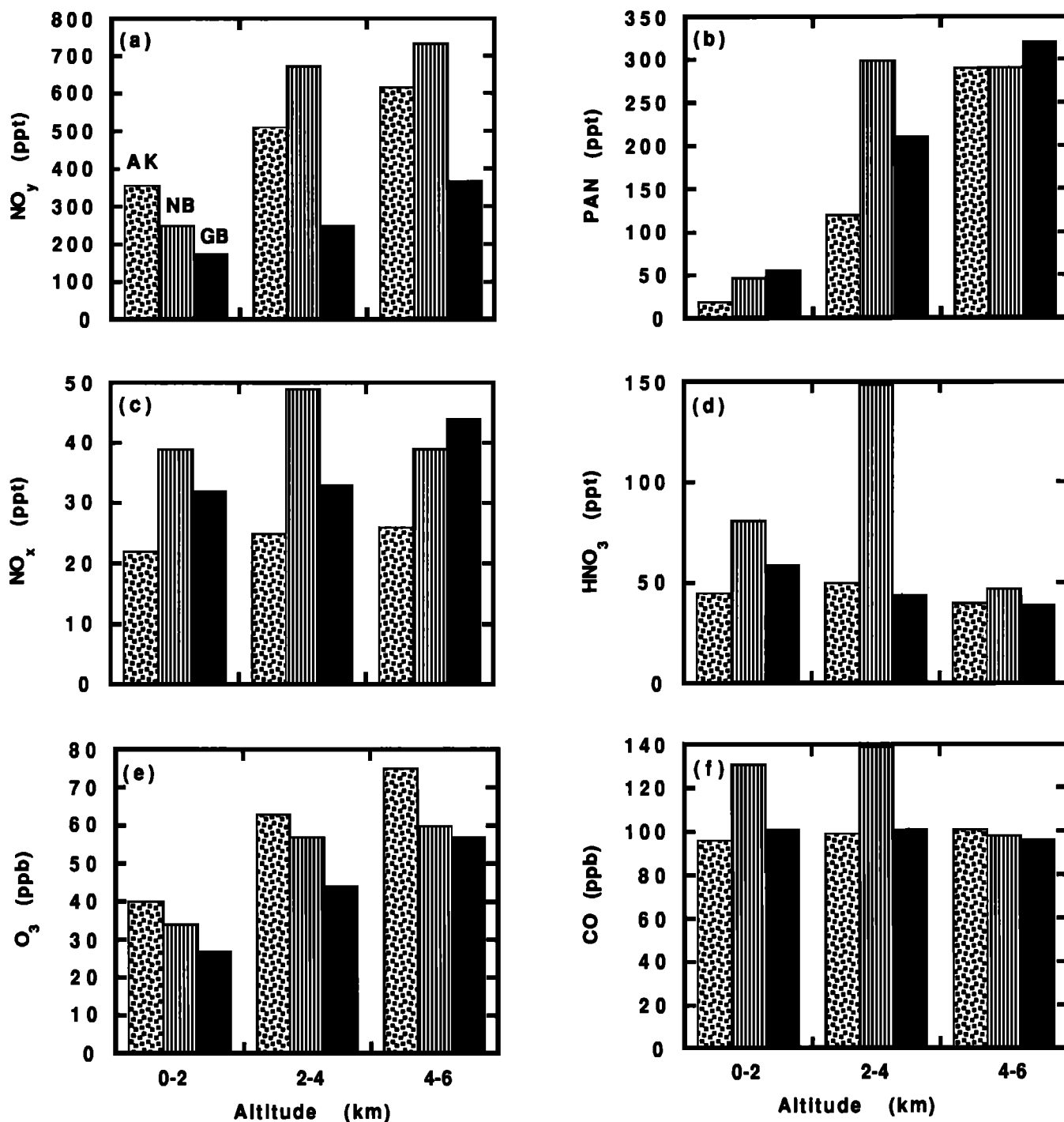


Fig. 7. A comparison of median mixing ratios of select species based on measurements in Alaska (AK; 50°-72°N), NB, and GB (ABLE3B) as a function of altitude.

deficiency of 25-50% has now been observed nearly everywhere in the remote atmospheres of the northern hemisphere and has been used to infer the ubiquitous presence of unknown reactive nitrogen species [Fahey *et al.*, 1986; Calvert and Madronich, 1987; Singh, 1987; Roberts, 1990; Ridley, 1991; Sandholm *et al.*, 1992; Singh *et al.*, 1992b; Atlas *et al.*, 1992]. Independent measurements of organic nitrates have been able to account for a very small fraction of total reactive nitrogen [Buhr *et al.*, 1990; Atlas *et al.*, 1992]. It is pertinent to add that this deficiency is virtually

nonexistent in semipolluted environments where these nitrogen species are able to account for all of  $\text{NO}_y$  [Parrish *et al.*, 1993]. Goose Bay ABLE3B measurements are the first to find near accountability in the reactive nitrogen budget at a remote site. Figure 11 shows a comparison of mean fractional ( $\text{NO}_{y_i}/\text{NO}_y$ ) and actual ( $\text{NO}_y - \text{NO}_{y_i}$ ) odd nitrogen deficiency as measured in Alaska, NB, and GB. It is noted that the fractional accountability of reactive nitrogen over eastern Canada was generally better than that over Alaska.

One explanation for the balanced nitrogen budget at GB

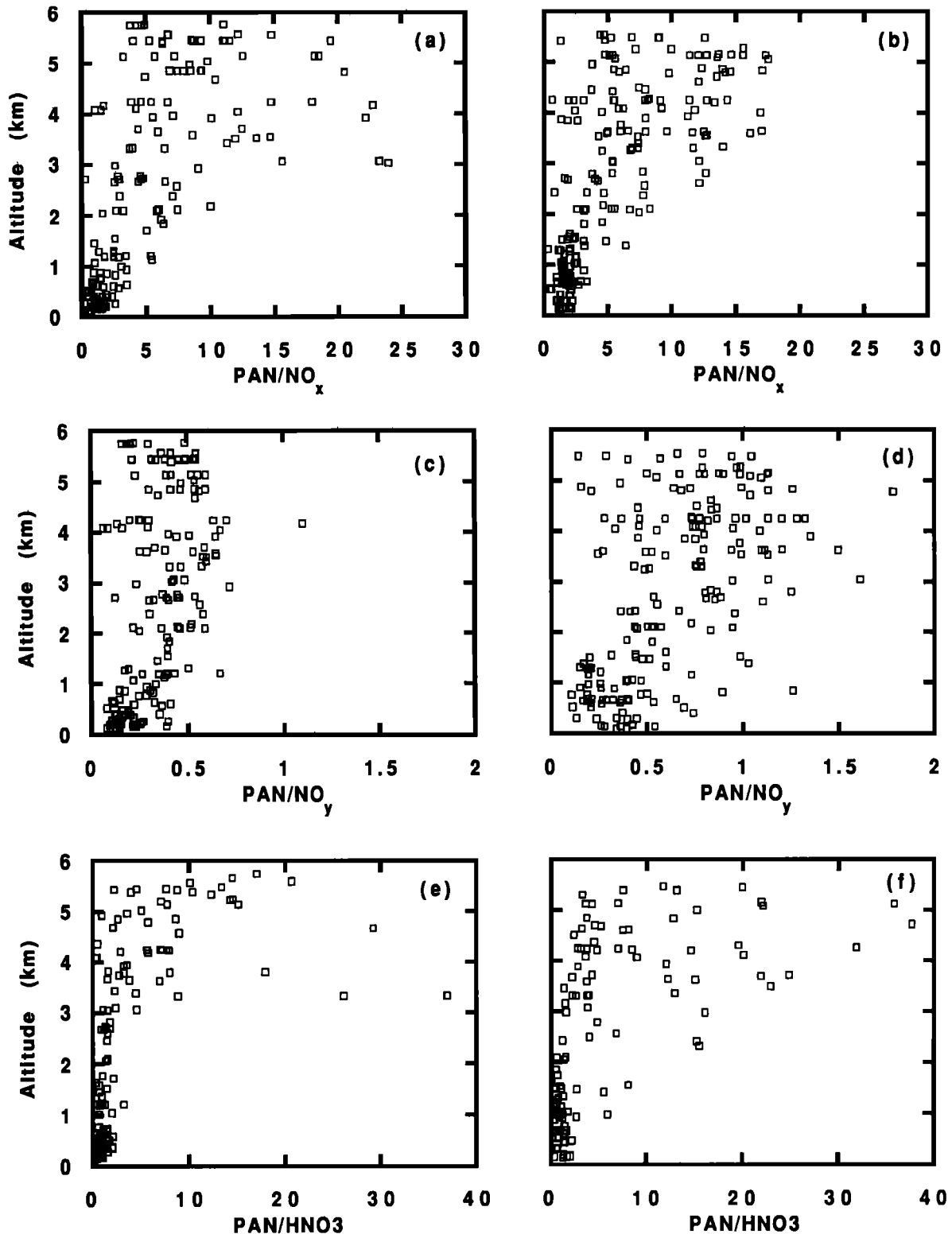


Fig. 8. Vertical distribution of PAN/NO<sub>x</sub>, PAN/NO<sub>y</sub>, and PAN/HNO<sub>3</sub> in the high-latitude troposphere of eastern Canada for all (a, c, e) NB and (b, d, f) GB missions. PAN/NO<sub>y</sub> exceeding 1 were sometimes seen during GB missions 16-19. This was occasionally also true of HNO<sub>3</sub>/NO<sub>y</sub> ratios during the GB series.

may be due to the fact that the air masses are greatly influenced by fresh emissions and not much oxidation has occurred. This would imply young air masses akin to those encountered in urban areas where essential balance is frequently observed [Parrish *et al.*, 1993]. However, this

would imply higher rather than lower hydrocarbon and NO<sub>y</sub> abundances and this was generally not the case. Another possibility may be that instrumental errors lead to low NO<sub>y</sub> or high PAN or HNO<sub>3</sub> measurements. The possibility of instrumental problems was considered by all investigators,

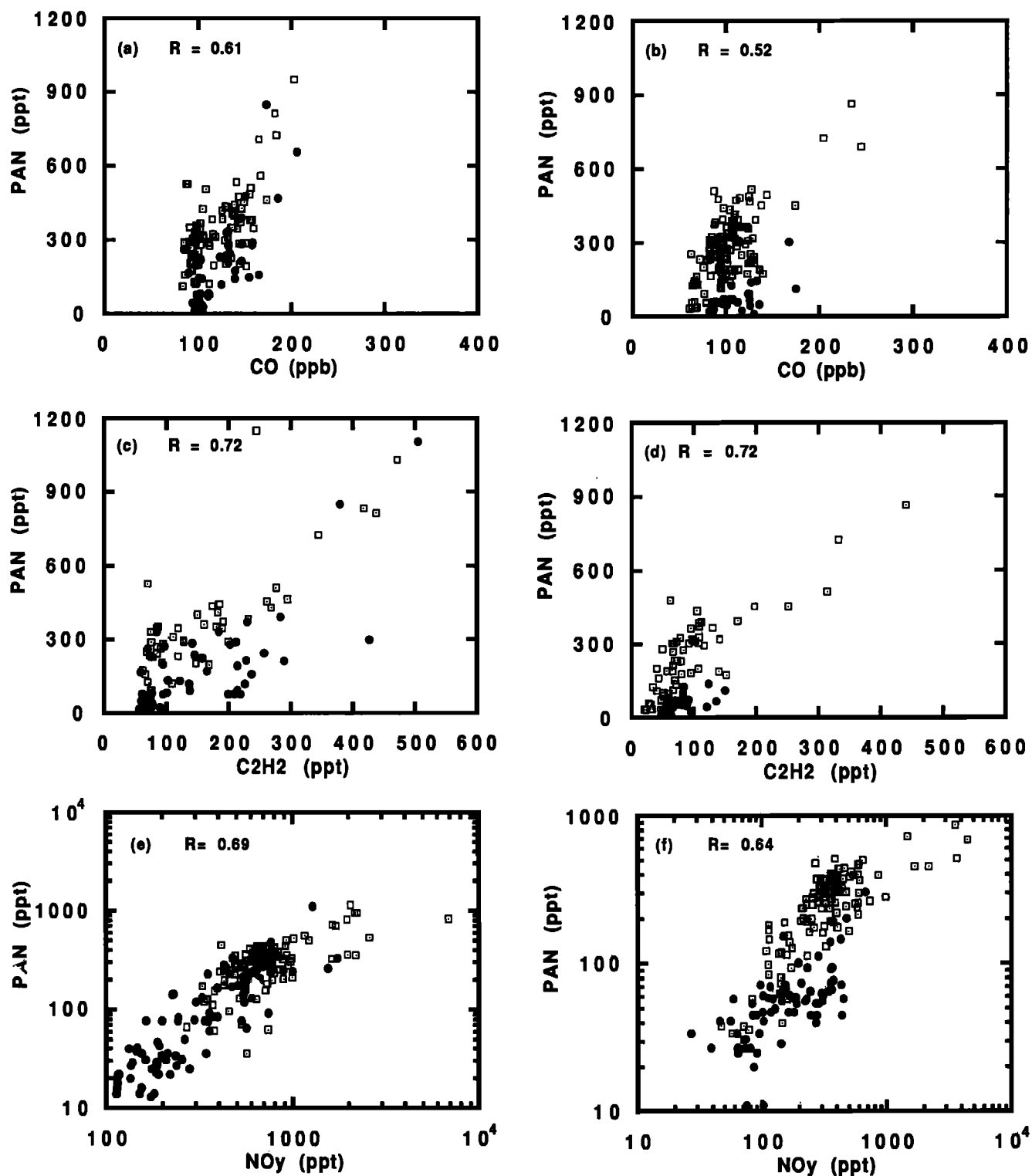


Fig. 9. Correlation of PAN mixing ratios with those of selected chemicals (CO, C<sub>2</sub>H<sub>2</sub>, and NO<sub>y</sub>) for (a, c, e) NB and (b, d, f) GB measurements. Circles and squares show data collected below and above 2-km altitude, respectively. All correlation coefficients are based on a linear fit.

but no unusual behavior could be found until mission 21. After mission 21, NO<sub>y</sub> measurements were reported only as lower limits due to possible contamination of the NO<sub>y</sub> converter [Sandholm *et al.*, this issue]. Because of the low free tropospheric NO<sub>y</sub> the smaller NO<sub>y</sub>/O<sub>3</sub> ratio at GB compared to NB and some instances of PAN and HNO<sub>3</sub> exceeding NO<sub>y</sub>, an

attempt was made to compare Schefferville tower NO<sub>y</sub> data (0.03 km above ground level), where NO<sub>y</sub> was measured with a chemiluminescence instrument, with that of aircraft data during periods of over flight (0.1–1 km above ground level). Table 4 summarizes these results. This comparison was made greatly difficult because of the presence of highly variable but

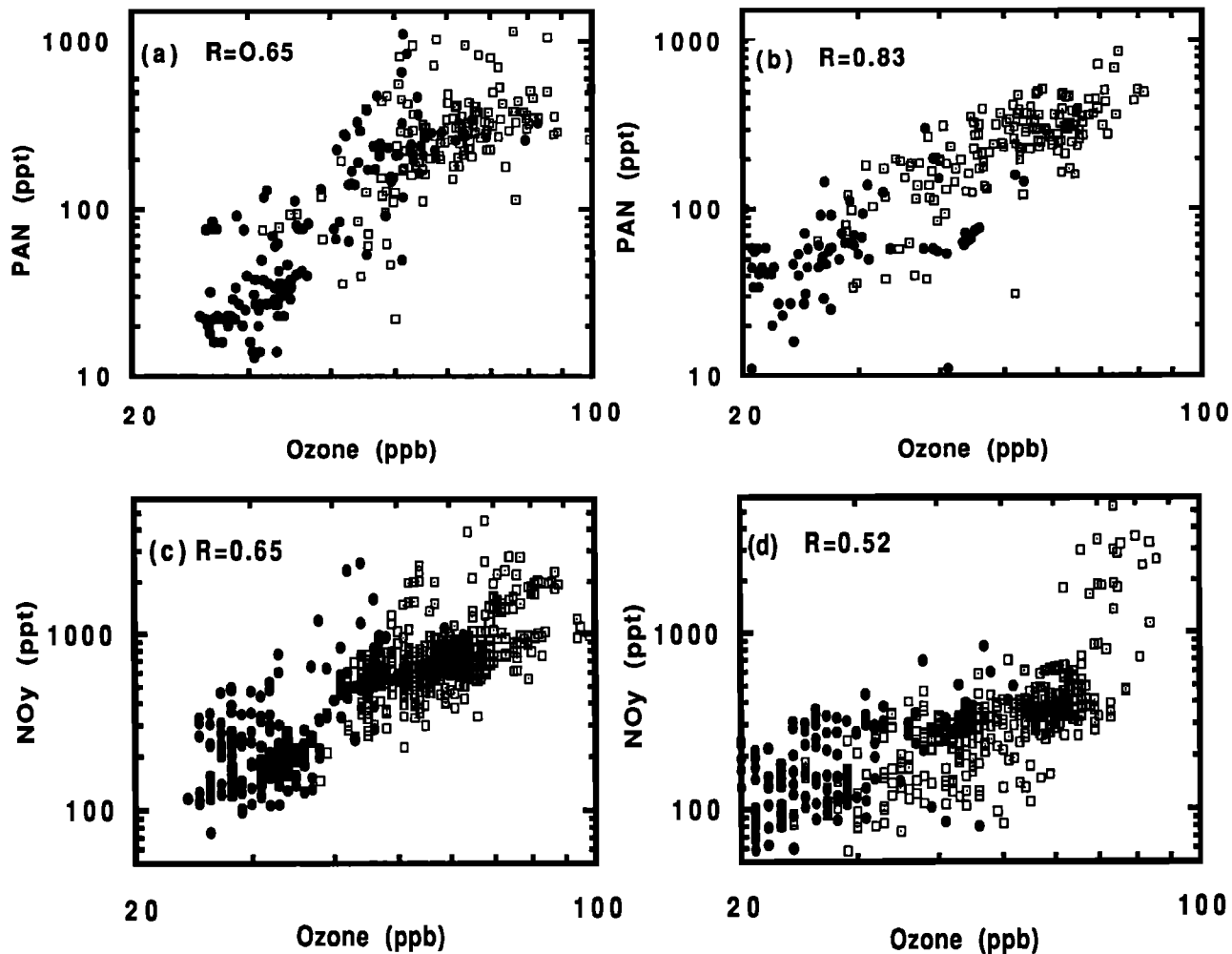


Fig. 10. Correlation of PAN and  $\text{NO}_y$  mixing ratios with ozone for (a,c) NB and (b,d) GB data.  $\text{NO}_y$  and  $\text{O}_3$  data are 3-min averages. Same as in Figure 8.

substantial nitrate aerosol concentrations (2-180 ppt) at the tower site [Talbot *et al.*, this issue; Gorzelska *et al.*, this issue]. No size fractionation was done; however, high nitrate concentrations are often associated with fresh sources and can be expected to be in the fine aerosol fraction. An unknown but large fraction of this aerosol  $\text{NO}_3^-$  was probably sampled by the tower instrument as  $\text{NO}_y$ . Unfortunately, aerosol nitrate data at the tower site were available during only one of the four overflight periods (mission 11). The data from tower and aircraft for mission 11 were found to be in reasonable agreement. Table 4 data in no way contradict the finding by Sandholm *et al.* [this issue] that the  $\text{NO}_y$  instrument was behaving as expected.

#### Role of PAN as a Source of $\text{NO}_x$ and $\text{O}_3$

Data presented here show that significant mixing ratios of PAN and correspondingly small mixing ratios of  $\text{NO}_x$  coexist in the troposphere over eastern Canada. Whereas combustion sources of  $\text{NO}_x$  were clearly present, a certain fraction could also be produced from the PAN reservoir. During the ABLE3A Alaska effort it was calculated that 50 to 70% of the median  $\text{NO}_x$  mixing ratios present could have come from the PAN reservoir alone [Jacob *et al.*, 1992; Singh *et al.*, 1992b]. What fraction of the available  $\text{NO}_x$  could have come from PAN decomposition source alone in NB and GB during ABLE3B?

To explore this possibility, a one-dimensional model of NMHC- $\text{O}_3$ - $\text{NO}_x$  photochemistry in the troposphere was adapted to the physical and chemical environment encountered during ABLE3B (August 1, 50°N) and a calculation similar to that in the work of Singh *et al.* [1992b] was performed. In comparison to the previous effort, larger K values (by a factor of 2) were used in the present computations, as these values provided a better fit to measured PAN and  $\text{O}_3$ , especially in the lower troposphere. Mean atmospheric temperature as well as mixing ratios of key species were chosen so as to reproduce the mean observed values during ABLE3B (e.g., 400 ppt for PAN and 60 ppb for  $\text{O}_3$  at 6 km). Model simulations, under clear sky conditions, were run when all sources of  $\text{NO}_x$  (e.g., lightning, soil) were set equal to zero and zero flux was assumed for NO,  $\text{NO}_2$ ,  $\text{HNO}_3$ , and  $\text{HO}_2\text{NO}_2$  at the upper boundary of the model. Constant deposition velocities were assumed for these gases at the ground. Surface NMHC ( $\text{C}_2$  to  $\text{C}_4$  NMHC) mixing ratios were set equal to the mean measured values [Blake *et al.*, this issue].

Results from this one-dimensional model simulation are shown in Figure 12. Also shown in Figure 12 are the median values of the observed  $\text{NO}_x$  mixing ratios both at NB and GB. Given the assumed PAN profile, nearly 15 to 20 ppt of  $\text{NO}_x$ , depending on altitude, could result from decomposition of PAN alone. These simulations suggest that the PAN reservoir in the high-latitude troposphere could provide an important

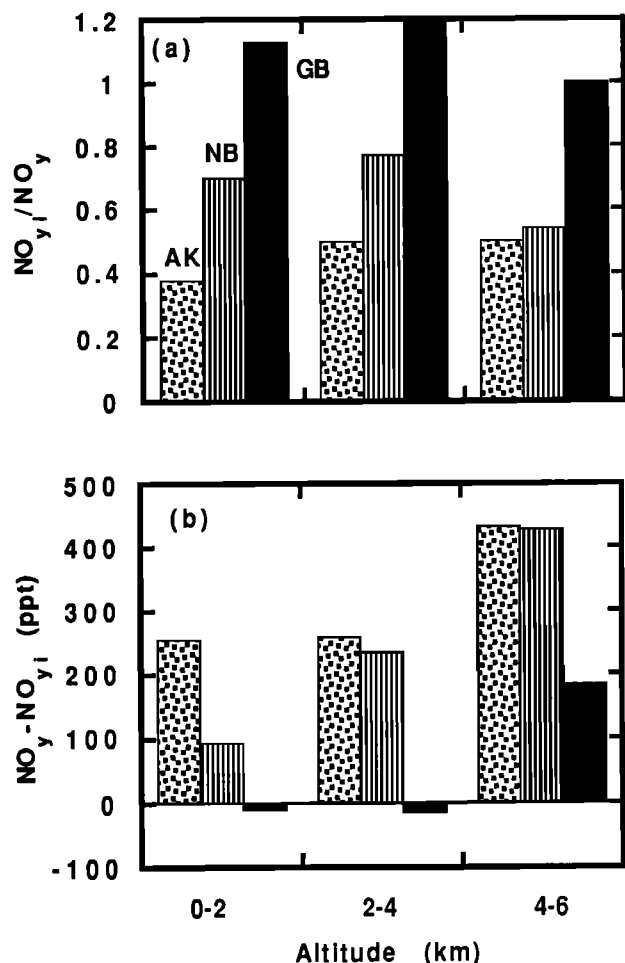


Fig. 11. A comparison of mean atmospheric reactive nitrogen budget based on measurements in Alaska (AK), NB, and GB (ABLE3B) as a function of height.

baseline source of local  $NO_x$  and hence could contribute to  $O_3$  production.

Was there sufficient  $NO_x$  present in the atmosphere over eastern Canada to cause net  $O_3$  synthesis? The  $(NO_x)_{eq}$  value (dashed curve in Figure 12) is calculated based on chemistry previously described by Singh *et al.*, [1992b] and a faster diffusion as stated above. The latter change had the effect of increasing calculated  $NO_x$  and  $(NO_x)_{eq}$  in the lower troposphere. Figure 12 shows that 25 to 45 ppt of  $NO_x$  is

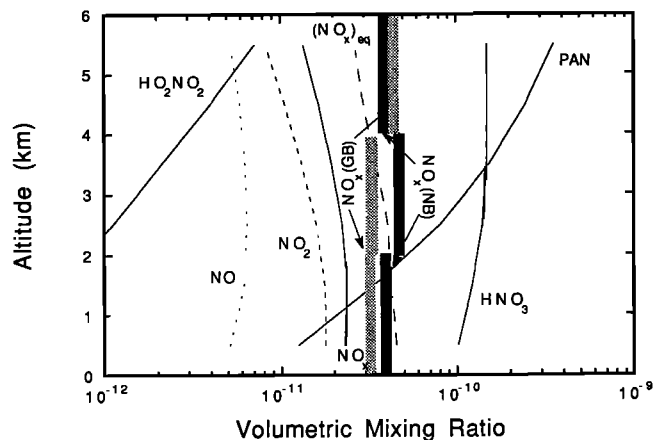


Fig. 12. Steady state odd nitrogen species distribution due to an imposed PAN source as calculated with a one-dimensional model. In this model run, all direct sources of  $NO_x$  (lightning, stratospheric flux, and soil) are set to zero. PAN and  $O_3$  are set to 400 parts per trillion (ppt) and 60 ppb, respectively, at 6 km. Model is exercised at  $50^\circ N$  (August 1) under clear sky conditions and assumes many of the mean features observed during ABLE3B. The dashed curve  $\{NO_x\}_{eq}$  indicates the amount of  $NO_x$  needed to balance the photochemical production and destruction rates of  $O_3$ . Shaded bars show median  $NO_x$  values observed at NB and GB.

needed for a net equilibrium between  $O_3$  production and loss processes. The  $NO_x$  provided by the PAN reservoir is about half the equilibrium value. The measured median  $NO_x$  mixing ratios are typically above this level throughout much of the troposphere sampled at NB. Thus it appears that net photochemical  $O_3$  production may be occurring at NB. This is not always the case at GB where median  $NO_x$  values in the lower troposphere are below the calculated  $(NO_x)_{eq}$  values. In the absence of the PAN reservoir, median  $NO_x$  mixing ratios would be lower resulting in greater photochemical  $O_3$  destruction.

## CONCLUSIONS

The two field studies performed over Alaska and eastern Canada have shown that large abundances of PAN and  $NO_y$  are present in the Arctic/subarctic troposphere of the northern hemisphere during the summer. Coincident PAN and  $O_3$  atmospheric structures suggest that continental precursors define the behavior of both PAN and  $O_3$ . In the free troposphere, PAN was found to be the single most abundant

TABLE 4. A Comparison of Aircraft and Tower  $NO_y$  Measurements Near the Schefferville Site During ABLE3B

Quantity	Altitude, km	Mission			
		11	14	15	17
$NO_y^*$ , ppt	0.03 AGL (tower)	400	240	275	195
$NO_y^+$ ppt	0.1 - 1 AGL (aircraft)	300	130	220	114
$NO_3^-$ ppt	0.03 (tower)	112	ND†	ND	ND
$NO_y^*/NO_y^+$		1.32 (U)† 0.96 (C)	1.83 (U) ----(C)	1.25 (U) ----(C)	1.7 (U) ----(C)

\*Harvard tower data. Aerosol  $NO_3^-$  was measured in the 2-to 180-ppt range ( $46 \pm 53$  ppt) from July 22 to August 3, 1991, at the 0.03-km tower level by University of New Hampshire. AGL: Above ground level.

†GIT aircraft data.  $NO_3^-$  is very low ( $\approx 5\%$  of  $NO_y$ ) and is expected to be largely in the coarse aerosol fraction which is probably not sampled.

†ND, no data; U, uncorrected for  $NO_3^-$ ; C, corrected data assuming that all  $NO_3^-$  is sampled by the tower instrument as  $NO_y$ .

reactive nitrogen species constituting a major fraction of  $\text{NO}_y$  and was significantly more abundant than  $\text{NO}_x$  and  $\text{HNO}_3$ . The nitrogen budget based on missions conducted from the North Bay site showed a shortfall, as expected, but a similar budget from the Goose Bay operations showed essential balance, contrary to what has been previously reported from remote locations. At remote locations, reservoir species such as PAN have the ability to provide an important source of  $\text{NO}_x$ . Meteorological considerations as well as relationships between reactive nitrogen and anthropogenic tracer species suggest that the atmosphere over eastern Canada during ABLE3B was strongly influenced by forest fires and transported industrial pollution.

**Acknowledgments.** This research was supported by the NASA Global Tropospheric Experiment. We acknowledge all ABLE3B participants for their cooperation and support. Special thanks are due to the flight and ground crew of the Wallops Electra for making this effort a success. We greatly appreciate the computational assistance provided by B. Sitton of the Synernet Corporation and data interpretation by W. Viezee of SRI International.

#### REFERENCES

- Anderson, B. E., G. L. Gregory, J. D. W. Barrick, J. E. Collins, and G. W. Sachse, Summertime tropospheric ozone distributions over central and eastern Canada, *J. Geophys. Res.*, this issue.
- Atlas, E. et al., Partitioning and budget of  $\text{NO}_y$  species during MLOPEX, *J. Geophys. Res.*, **97**, 16,449-16,462, 1992.
- Barrie, L. A., Arctic air pollution: An overview of current knowledge, *Atmos. Environ.*, **20**, 643-663, 1986.
- Blake, D. R. T. W. Smith, T.-Y. Cheng, W. J. Whipple, and F. S. Rowland, Effects of biomass burning on summertime nonmethane hydrocarbon concentrations in the Canadian wetlands, *J. Geophys. Res.*, this issue.
- Browell, E. V., M. A. Fenn, C. F. Butler, W. B. Grant, R. C. Harriss, and M. C. Shipham, Ozone and aerosol distributions in the summertime troposphere over Canada, *J. Geophys. Res.*, this issue.
- Buhr, M. P., D. D. Parrish, R. B. Norton, F. C. Fehsenfeld, and R. C. Seivers, Contribution of organic nitrates to the total reactive nitrogen budget at a rural eastern U.S. site, *J. Geophys. Res.*, **95**, 9809-9816, 1990.
- Calvert, J. G., and S. Madronich, Theoretical study of the initial products of atmospheric oxidation of hydrocarbons, *J. Geophys. Res.*, **92**, 2211-2220, 1987.
- Crutzen, P. J., The role of  $\text{NO}$  and  $\text{NO}_2$  in the chemistry of the troposphere and stratosphere, *Ann. Rev. Earth Planet Sci.*, **7**, 443-472, 1979.
- Fahey, D. W., G. Hübler, D. D. Parrish, E. J. Williams, R. B. Norton, B. A. Ridley, H. B. Singh, S. C. Liu, and F. C. Fehsenfeld, Reactive nitrogen species in the troposphere: Measurements of  $\text{NO}$ ,  $\text{NO}_2$ ,  $\text{HNO}_3$ , particulate nitrate, peroxyacetyl nitrate (PAN),  $\text{O}_3$ , and total reactive odd nitrogen ( $\text{NO}_y$ ) at Niwot Ridge, Colorado, *J. Geophys. Res.*, **91**, 9781-9793, 1986.
- Gozelska, K., et al., Chemical composition of the atmospheric aerosol in the troposphere over the Hudson Bay lowlands and Quebec-Labrador regions of Canada, *J. Geophys. Res.*, this issue.
- Global Tropospheric Experiment (GTE), GTE/ABLE3B expedition, Aircraft navigational and meteorological data, GTE Proj. Off., Hampton, Virginia, 1990.
- Harriss, R. C. et al., The Arctic Boundary Layer Expedition (ABLE3A): July-August 1988, *J. Geophys. Res.*, **97**, 16,383-16,394, 1992.
- Harriss, R. C., et al., The Arctic Boundary Layer Expedition (ABLE3B): July-August 1990, *J. Geophys. Res.*, this issue.
- Jacob, D., et al., Summertime photochemistry of the troposphere at high northern latitudes, *J. Geophys. Res.*, **97**, 16,421-16,432, 1992.
- Jaffe, D. A., Honrath, R. E., J. A. Herring, S. M. Li, and J. D. Kahl, Measurements of nitrogen oxides at Barrow, Alaska, during spring: Evidence for regional and northern hemispheric sources of pollution, *J. Geophys. Res.*, **96**, 7395-7405, 1991.
- Joos, L. F., W. F. Landolt, and H. Leuenberger, Calibration of peroxyacetyl nitrate measurements with an  $\text{NO}_x$  analyzer, *Environ. Sci. Technol.*, **20**, 1269-1273, 1986.
- Kanakidou, M., H. B. Singh, K. M. Valentin, and P. J. Crutzen, A two-dimensional model study of ethane and propane oxidation in the troposphere, *J. Geophys. Res.*, **96**, 15, 395-15,413, 1991.
- Levy, H., II, Normal atmosphere: Large radical and formaldehyde mixing ratios predicted, *Science*, **173**, 141-143, 1971.
- Logan, J. A., M. J. Prather, S. C. Wofsy, and M. B. McElroy, Tropospheric chemistry: A global perspective, *J. Geophys. Res.*, **86**, 7210-7254, 1981.
- McNeal, R. J., J. P. Mugler, Jr., R. C. Harriss, and J. M. Hoell, Jr., NASA Global Tropospheric Experiment, *EOS Trans. AGU*, **64**, 561-562, 1983.
- Murphy, D. M., et al., Reactive nitrogen and its correlation with ozone in the lower stratosphere and upper troposphere, *J. Geophys. Res.*, **98**, 8751-8773, 1993.
- Parrish, D., et al., The total reactive oxidized nitrogen levels and the partitioning between the individual species at six rural sites in eastern North America, *J. Geophys. Res.*, **98**, 2927-2939, 1993.
- Rahn, K. A., Progress in Arctic air chemistry, 1980-1984, *Atmos. Environ.*, **19**, 1987-1994, 1985.
- Ridley, B. A., et al., Ratios of peroxyacetyl nitrate to active nitrogen observed during aircraft flights over the eastern Pacific Ocean and continental United States, *J. Geophys. Res.*, **95**, 10,179-10,192, 1990.
- Ridley, B. A., Recent measurements of oxidized nitrogen compounds in the troposphere, *Atmos. Environ.*, **25**(A), 1905-1926, 1991.
- Roberts, J. M., The atmospheric chemistry of organic nitrates, *Atmos. Environ.*, **24**(A), 243-287, 1990.
- Sandholm, S., J. D. Bradshaw, K. S. Dorris, M. O. Rogers, and D. D. Davis, An airborne compatible photofragmentation two-photon laser-induced fluorescence instrument for measuring background tropospheric  $\text{NO}$ ,  $\text{NO}_x$ , and  $\text{NO}_2$ , *J. Geophys. Res.*, **95**, 10,155-10,161, 1990.
- Sandholm, S., et al., Arctic tropospheric observations related to  $\text{N}_x\text{O}_y$  distributions: ABLE3A, *J. Geophys. Res.*, **97**, 16,481-16,510, 1992.
- Sandholm, S., et al., Summertime partitioning and budget of  $\text{NO}_y$  compounds in the troposphere over Alaska and Canada: ABLE3B, *J. Geophys. Res.*, this issue.
- Schnell, R. C., Arctic haze and the Arctic Gas and Aerosol Sampling Program (AGASP), *Geophys. Res. Lett.*, **11**, 361-364, 1984.
- Shipham, M. C., A. S. Bachmeier, D. R. Cahoon, G. L. Gregory, and E. V. Browell, A meteorological interpretation of the Arctic Boundary Layer Expedition (ABLE3B) flight series, *J. Geophys. Res.*, this issue.
- Singh, H. B., Reactive nitrogen in the troposphere, *Environ. Sci. Technol.*, **21**, 320-327, 1987.
- Singh, H. B., and P. L. Hanst, Peroxyacetyl nitrate (PAN) in the unpolluted atmosphere: An important reservoir for nitrogen oxides, *Geophys. Res. Lett.*, **8**, 941-944, 1981.
- Singh, H. B., and L. J. Salas, Methodology for the analysis of peroxyacetyl nitrate (PAN) in the unpolluted atmosphere, *Atmos. Environ.*, **17**, 1507-1516, 1983.
- Singh, H. B., et al., PAN measurements during CITE2: Atmospheric distribution and precursor relationships, *J. Geophys. Res.*, **95**, 10,163-10,178, 1990.
- Singh, H. B., et al., Atmospheric measurements of PAN and other organic nitrates at high latitudes: Possible sources and sinks, *J. Geophys. Res.*, **97**, 16,511-16,522, 1992a.
- Singh, H. B., et al., Relationship of PAN to active and total odd nitrogen at northern high latitudes: influence of reservoir species on  $\text{NO}_x$  and  $\text{O}_3$ , *J. Geophys. Res.*, **97**, 16,523-16,531, 1992b.
- Singh, H. B., D. O'Hara, D. Herlth, W. Sachse, D. R. Blake, J. D. Bradshaw, M. Kanakidou, and P. J. Crutzen, Acetone in the atmosphere: Distribution, sources, and sinks, *J. Geophys. Res.*, this issue.
- Talbot, R. W., A. S. Vijgen, and R. C. Harriss, Measuring tropospheric  $\text{HNO}_3$ : Problems and prospects for nylon filter and mist chamber techniques, *J. Geophys. Res.*, **95**, 7553-7561, 1990.
- Talbot, R. W., et al., Summertime distributions and relations of reactive oddnitrogen species and  $\text{NO}_y$  in the troposphere over Canada, *J. Geophys. Res.*, this issue.
- Wofsy, S. C., et al., Atmospheric chemistry in the Arctic and subarctic: Natural fires, mid-latitude industrial sources, and stratospheric inputs, *J. Geophys. Res.*, **97**, 16,731-16,746, 1992.
- Wofsy, S. C., et al., Factors influencing atmospheric subarctic North America during summer, *J. Geophys. Res.*, this issue.

---

D. R. Blake, University of California, Irvine, CA 92717.  
J. D. Bradshaw and S. T. Sandholm, Georgia Institute of  
Technology, Atlanta, GA 30332.  
G. L. Gregory and G. W. Sachse, NASA Langley Research Center,  
Hampton, VA 23665.  
D. Herlth and H. B. Singh, NASA Ames Research Center, Moffett  
Field, CA 94035.

D. O'Hara, San Jose State University Foundation, Moffett Field,  
CA 94035.  
R. Talbot, University of New Hampshire, Durham, NH 03824.  
S. C. Wofsy, Harvard University, Cambridge, MA 02138.

**(Received May 12, 1992; revised March 12, 1993;  
accepted April 6, 1993.)**